

# NMR-monitored titration of acid-stress bacterial chaperone HdeA reveals that Asp and Glu charge neutralization produces a loosened dimer structure in preparation for protein unfolding and chaperone activation

McKinzie A. Garrison and Karin A. Crowhurst\*

Department of Chemistry and Biochemistry, California State University Northridge, 18111 Nordhoff St., Northridge, California 91330-8262

Received 9 November 2013; Revised 1 December 2013; Accepted 2 December 2013

DOI: 10.1002/pro.2402

Published online 4 December 2013 proteinscience.org

**Abstract:** HdeA is a periplasmic chaperone found in several gram-negative pathogenic bacteria that are linked to millions of cases of dysentery per year worldwide. After the protein becomes activated at low pH, it can bind to other periplasmic proteins, protecting them from aggregation when the bacteria travel through the stomach on their way to colonize the intestines. It has been argued that one of the major driving forces for HdeA activation is the protonation of aspartate and glutamate side chains. The goal for this study, therefore, was to investigate, at the atomic level, the structural impact of this charge neutralization on HdeA during the transition from near-neutral conditions to pH 3.0, in preparation for unfolding and activation of its chaperone capabilities. NMR spectroscopy was used to measure  $pK_a$  values of Asp and Glu residues and monitor chemical shift changes. Measurements of  $R_2/R_1$  ratios from relaxation experiments confirm that the protein maintains its dimer structure between pH 6.0 and 3.0. However, calculated correlation times and changes in amide protection from hydrogen/deuterium exchange experiments provide evidence for a loosening of the tertiary and quaternary structures of HdeA; in particular, the data indicate that the dimer structure becomes progressively weakened as the pH decreases. Taken together, these results provide insight into the process by which HdeA is primed to unfold and carry out its chaperone duties below pH 3.0, and it also demonstrates that neutralization of aspartate and glutamate residues is not likely to be the sole trigger for HdeA dissociation and unfolding.

**Keywords:** HdeA; chaperone; acid-stress; NMR titration; pH titration; acid-dissociation constant; hydrogen exchange; correlation time; unfolding

---

*Abbreviations:* BC loop, the sequence of residues located between helices B and C in HdeA; CpHmd, constant pH molecular dynamics; HSQC, heteronuclear single quantum coherence; PF, protection factor;  $pK_a$ , negative log value of the acid dissociation constant; TOCSY, Total Correlation Spectroscopy.

Additional Supporting Information may be found in the online version of this article.

Grant sponsor: NSF; Grant number: CHE-1040134. Grant sponsor: College of Science and Mathematics at CSU Northridge.

\*Correspondence to: Karin Crowhurst, Department of Chemistry and Biochemistry, California State University Northridge, 18111 Nordhoff St., Northridge, CA, 91330-8262. E-mail: karin.crowhurst@csun.edu

## Introduction

The low pH environment of the human stomach, which generally ranges from pH 1 to 3, acts as a defensive barrier against infection of the intestines by pathogenic bacteria.<sup>1</sup> The acidity of the stomach can cause aggregation of periplasmic proteins in gram-negative bacteria, effectively preventing normal bacterial function and often resulting in cell death.<sup>1,2</sup> When the low-pH obstacle fails the resulting gastrointestinal colonization produces dysentery, a condition characterized by hemorrhagic diarrhea estimated to be responsible for the deaths of at least 800,000 children per year.<sup>3</sup>

The vulnerability of the periplasmic proteins in bacteria results from their open exposure to the environment: porins on the outer surface of the organism permit small molecules, including protons, to flow into the periplasmic space.<sup>4,5</sup> Proteins in this region are therefore rapidly exposed to the low pH of the stomach, frequently resulting in protein unfolding and aggregation. Some pathogenic bacteria (including *Escherichia coli*, *Shigella flexneri* and *Brucella abortus*) have evolved an effective mechanism to prevent this aggregation by expressing the small chaperone protein HdeA. This 9.7 kDa protein, containing four helices (A–D) per monomer (Fig. 1), exists as an inactive dimer in environments above pH 3.0. The dimer interface is held together primarily by hydrophobic interactions from residues located on helix B.<sup>6</sup> It has been suggested that the loop region between helices B and C, containing negatively charged glutamate and aspartate residues, also help to stabilize the dimer at higher pH values

by forming salt bridges with lysines on the opposing monomer.<sup>7</sup>

A very acidic environment (pH < 3), such as that found in the stomach, results in the protonation of the sixteen Glu and Asp residues spread throughout HdeA, thereby eliminating many of the electrostatic interactions with lysines that maintain the folded dimer structure.<sup>2</sup> This is believed to trigger exposure of the hydrophobic interface, which ultimately leads to the formation of an unfolded, active monomer capable of associating with other periplasmic proteins via hydrophobic interactions.<sup>2</sup> Positively charged Lys residues, situated mostly at the N- and C-termini of the chaperone, allow for the HdeA-substrate complex to maintain solubility.<sup>1,2,8</sup> The transition between inactive dimer and active monomer has been characterized as ATP-independent, fast, and reversible. An increase in pH upon bacterial entry into the gastrointestinal tract has been shown to result in the slow release of the substrate proteins and the refolding of HdeA to its inactive dimer conformation.<sup>8</sup>

Researchers are motivated to characterize the mechanism by which HdeA becomes activated in order to improve targeting for vaccines or other therapeutics that can disable its activities and thereby weaken the infectivity of pathogenic bacteria. While several studies have been published that investigate biophysical properties of HdeA using a variety of techniques,<sup>1,7–10</sup> and although a crystal structure of the folded dimer is available,<sup>6</sup> there is still a lack of detailed atomic-level information about HdeA activity, and a deficiency in the number of pH

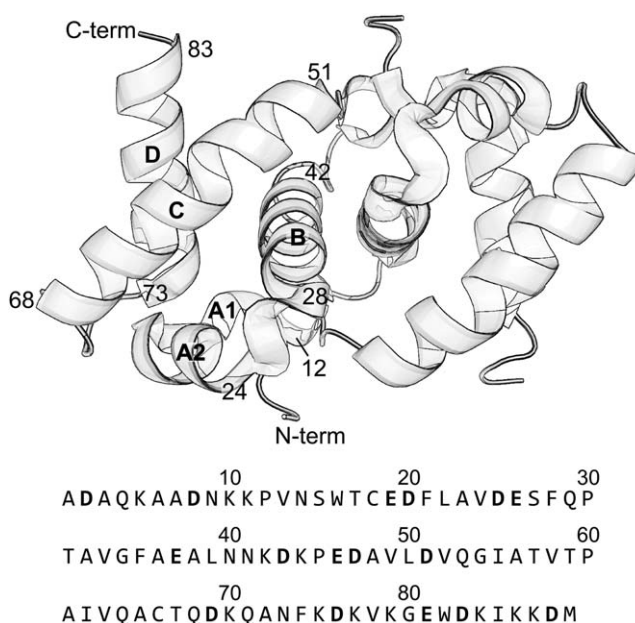


**Figure 1.** Ribbon diagram and sequence of HdeA. The crystal structure of the HdeA homodimer (PDB ID: 1DJ8) was previously solved.<sup>6</sup> The N- and C-termini for helices A–D are labeled for one monomer. The positions of aspartate and glutamate residues in the sequence are highlighted in boldface.

values used to collect data. NMR spectroscopy is an ideal choice for studying the transition of HdeA from folded, inactive dimer at neutral pH to unfolded, active monomer at low pH: NMR permits detailed characterization of the protein with atomic resolution, and the solution state conditions are exquisitely sensitive to disruptions within the protein, even with small step changes in pH.

It has already been mentioned that HdeA activation depends, in part, on the protonation of Asp and Glu residues with increasing acidity; until now, the  $pK_a$ s for these residues had been estimated through simulation.<sup>7</sup> There is a question, however, about whether this charge neutralization is the primary trigger for protein unfolding and activation, or whether it is only one of several contributing factors. The overall goal of these studies is to better describe the extent of the structural impact of neutralizing the Asp and Glu charges with lowered pH, and how it contributes to priming the protein for activation of its chaperone activities.

In this article we present experimental characterization of those  $pK_a$  values as part of a titration experiment between pH 6.0 and 3.0 that also followed the backbone chemical shift changes at each amino acid in the sequence. Total correlation spectroscopy (TOCSY) experiments were used to obtain  $pK_a$ s for all eleven aspartate and four out of five glutamate residues, and  $^1\text{H}$ - $^{15}\text{N}$  HSQC experiments were recorded to monitor backbone chemical shift changes. Considering that molecular motions often play significant roles in protein functionality, we were also interested in monitoring HdeA backbone dynamics to gain insight into the conformational and flexibility changes that take place due to Asp and Glu charge neutralization. Hydrogen/deuterium exchange and backbone relaxation experiments were recorded to describe these motions. Our studies have confirmed that HdeA maintains its dimer structure down to pH 3.0; notably, however, the structure becomes increasingly loosened as the pH is lowered and may participate in transient opening of the dimer prior to dissociation. We have also found that, although protonation of the aspartate and glutamate side chains heavily influence the changes in HdeA conformation and flexibility that take place in this preactivation state, it is also apparent that those influences are not sufficient to single-handedly initiate the full activation of HdeA into an unfolded monomeric state. Overall, these investigations of the correlation between ionization state, conformational changes and internal motions in the pH range 6.0–3.0 are critical to advance our understanding of the steps that are required to prime HdeA for unfolding, dissociation, and ultimate activation below pH 3.0. The design of future therapeutics will likely target the folded state of the protein; understanding the range of conformations available to HdeA between pH 6.0 and 3.0 may therefore be critical to this design process.

## Results

### Backbone amide chemical shift changes

Backbone chemical shifts were recorded via  $^1\text{H}$ - $^{15}\text{N}$  HSQC spectra (Fig. 2) and the weighted average of backbone  $^1\text{H}_\text{N}$  and  $^{15}\text{N}$  chemical shifts [ $\Delta_{\text{avg}}$ , see Eq. (1)] at each residue between pH 6.0 and 3.0 is plotted in Figure 3. It is clear from the results that most, if not all, of the larger chemical shift changes are directly influenced by the changes in ionization state for Asp and Glu residues. There are 31 residues whose overall chemical shifts are more than one standard deviation above the mean (excluding the 10% outliers). Of these, only eight (A6, V13, N14, T17, N40, V49, G54, and I85) are non-ionizable residues that are not directly adjacent to Asp or Glu in the sequence. Most of these residues can be found in helix A or in the region of the flexible segment between helices B and C (BC loop).

### Measurement of $pK_a$ values for Asp and Glu

There are no histidines or arginines in HdeA and the high  $pK_a$  for lysine side chains ensures that they are positively charged throughout the pH range being monitored. Thus, Asp and Glu residues are the only ionizable groups that are pH-dependent between 6.0 and 3.0. Considering that the protonation of these residues is believed to play a key role in the activation of HdeA's chaperone capabilities, it was important to measure their  $pK_a$ s. Three-dimensional TOCSY (C(CO)NH) experiments were used to monitor the pH-dependence of C $\beta$  and C $\gamma$  chemical shift changes from Asp and Glu residues, respectively, to obtain  $pK_a$  values. These carbons are directly adjacent to the carboxylic acid groups on the Asp and Glu side chains and are therefore sensitive reporters of the ionization states of these functional groups.

The experimentally measured Asp and Glu  $pK_a$  values and Hill coefficients are listed in Table I, along with their deviation from standard (random coil)  $pK_a$ s. Figure 4(a) provides examples of the quality of the fits to the titration curves for several residues. Equation (2) was used to fit each curve. Hill coefficient values calculated for the  $pK_a$  curve from each residue range from 0.88 to 1.23, with an average value of 1.05. Although most values are quite close to 1.00, residues with  $n < 1$  indicate a small amount of interference between the residue and an adjacent ionizable group, while those with  $n > 1$  indicate positive cooperativity.<sup>11,12</sup> Within the experimentally determined results, the average aspartate  $pK_a$  is 0.07 pH units from the standard value of 3.84,<sup>12</sup> with a range of 3.66–4.28, while the average measurable glutamate  $pK_a$  is only 0.01 pH units from the standard value of 4.32, with a range of 4.07–4.57.

Residue E37 is the only amino acid for which we could not confidently fit the data. The E37

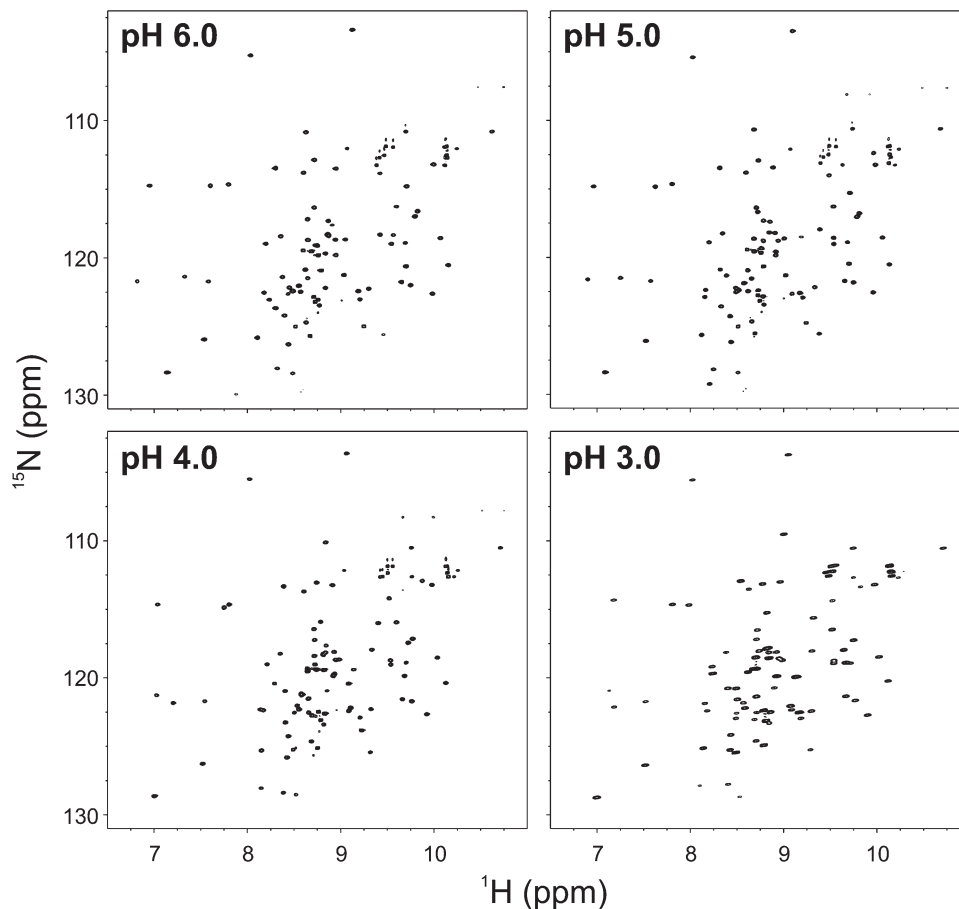


**Figure 2.**  $^1\text{H}$ - $^{15}\text{N}$  HSQCs, recorded between pH 6.0 and 3.0. All spectra are well-resolved and verify that the protein is fully folded throughout this pH range. Significant chemical shift changes are primarily the result of the change in ionization state of aspartate and glutamate side chains, which impact these residues as well as adjacent positions in the sequence.

titration curve is shown in Figure 4(b). Data at pH 2.6 and 2.8 were excluded due to overlap and low peak intensities, while no data could be obtained at

pH values above 5.0 because the required peaks were broadened and therefore unobservable. It seems clear from the plot in Figure 4(b) that, unlike

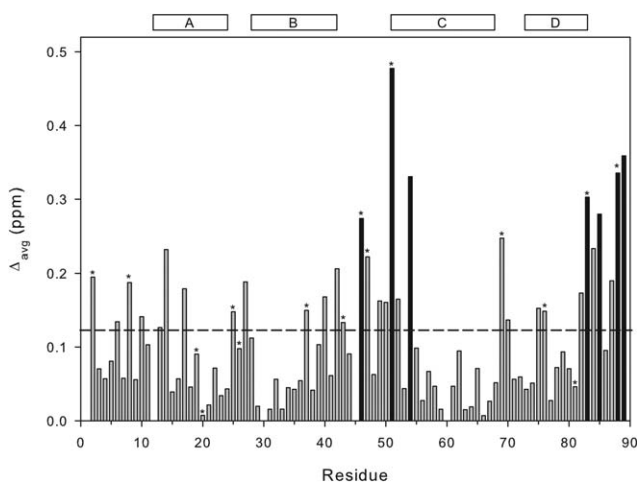


**Figure 3.** Backbone amide chemical shift change between pH 6.0 and 3.0. Bar chart shows the total amide chemical shift change ( $\Delta_{\text{avg}}$ ) over the pH range as a function of residue number. The term  $\Delta_{\text{avg}}$  is defined as a weighted function that includes both  $^1\text{H}_\text{N}$  and  $^{15}\text{N}$  backbone shifts, as per Eq. (1). Bars marked with (\*) indicate the positions of Asp and Glu residues in the sequence. The horizontal line indicates one standard deviation ( $1\sigma$ ) above the mean chemical shift (excluding the 10% outliers), and the black bars indicate residues with chemical shift changes more than  $3\sigma$  above the mean. Rectangles at the top of the graph indicate the positions of the helices within the folded protein.

**Table I.** Comparison of Experimentally Determined and Simulated  $pK_a$  Values for HdeA

Residue	Experimentally measured $pK_a \pm \text{error}$	Hill coefficient ( $n \pm \text{error}$ )	$\Delta(\text{exp} - \text{std}) pK_a^a$	Simulated dimer $pK_a$ (average) <sup>b</sup>	Simulated monomer $pK_a^b$
D2	$3.82 \pm 0.04$	$1.05 \pm 0.09$	-0.02	<sup>c</sup>	<sup>c</sup>
D8	$4.28 \pm 0.05$	$0.95 \pm 0.11$	0.44	<sup>c</sup>	<sup>c</sup>
E19	$4.38 \pm 0.04$	$1.07 \pm 0.12$	0.06	$3.7^d$	$3.8^e$
D20	$3.66 \pm 0.08$	$1.09 \pm 0.18$	-0.18	2.6	3.8
D25	$3.71 \pm 0.04$	$1.01 \pm 0.08$	-0.13	3.1	2.7
E26	$4.57 \pm 0.04$	$1.19 \pm 0.13$	0.25	4.35	4.0
E37	<sup>f</sup>			6.7	5.3
D43	$3.87 \pm 0.06$	$1.06 \pm 0.18$	0.03	2.85	3.7
E46	$4.07 \pm 0.03$	$1.03 \pm 0.08$	-0.25	3.45	3.7
D47	$4.14 \pm 0.06$	$0.88 \pm 0.11$	0.30	3.85	4.2
D51	$3.83 \pm 0.10$	$1.14 \pm 0.24$	-0.01	2.8	3.8
D69	$3.74 \pm 0.07$	$1.23 \pm 0.23$	-0.10	3.5	3.8
D76	$3.75 \pm 0.04$	$1.00 \pm 0.08$	-0.09	2.75	3.5
E81	$4.23 \pm 0.03$	$1.00 \pm 0.08$	-0.09	4.1	4.0
D83	$3.97 \pm 0.07$	$0.94 \pm 0.13$	0.13	3.1	3.7
D88	$4.25 \pm 0.04$	$1.09 \pm 0.12$	0.41	<sup>c</sup>	<sup>c</sup>

<sup>a</sup> Difference between experimental and standard  $pK_a$ s. Standard values used: Asp = 3.84 and Glu = 4.32.<sup>12</sup>

<sup>b</sup> Reprinted with permission from Zhang et al.<sup>7</sup> Copyright 2011, American Chemical Society.

<sup>c</sup> Simulations were based on the crystal structure, which included only residues 9–87 due to disorder at the N- and C-termini.

<sup>d</sup> Values in this column are averaged from simulated  $pK_a$ s reported for each monomer within the crystal structure of the HdeA dimer.<sup>7</sup>

<sup>e</sup> Values in this column based on theoretical monomer structure.<sup>7</sup>

<sup>f</sup> Value poorly fit—see main text for discussion.

all the other acidic residues, the upper plateau of the curve is likely to be higher than pH 6.0. Since we do not know the position of that upper plateau we cannot confidently fit the data, but we estimate the  $pK_a$  for E37 to be  $> 5.0$ . This estimate is consistent with the simulated data (see Table I),<sup>7</sup> which predicts that E37 has a significantly higher  $pK_a$  than any other acidic amino acid in the protein.

### Hydrogen/deuterium exchange experiments

In an effort to monitor changes in conformation and/or dimer stability in HdeA with decreasing pH and change in net protein charge, a set of hydrogen/deuterium exchange experiments were performed and monitored by NMR. HdeA was rapidly exchanged into 50 mM citrate buffer in 100%  $^2\text{H}_2\text{O}$  at pH 3.0, 4.0, 5.0, and 6.0, and SOFAST-HSQC experiments were recorded over a 12-h period. While Supporting Information Figure S1 provides quantitative information with plots illustrating protection factors (PFs) at each pH as well as changes in PF between each unit, Figure 5 illustrates a simplified analysis of the hydrogen/deuterium exchange experiments indicating the residues for which peaks are visible in the HSQCs at the start and end of each experiment. The results from Figure 5 show a clear, progressive decrease in solvent protection in HdeA with lowered pH. In particular, very few backbone amide groups show evidence for stable protection after 12 h at pH 3.0. However, it is notable that residues 4, 7, 10, and 11 have a greater degree of protection from

solvent at pH 4.0 and 3.0 compared with pH 6.0 and 5.0 (Fig. 5 and Supporting Information S1). Overall, solvent protection for the A1 helix is quite poor at all pH values, indicating that this helix may be conformationally dynamic. The results are similar for the N-terminal segment of helix C, the C-terminal segment of helix D and the BC loop.

### Calculated correlation times from $R_2/R_1$ ratios

$R_1$  and  $R_2$  relaxation experiments were recorded on HdeA at pH 3.0, 4.0, 5.0, and 6.0 in order to obtain preliminary data on areas of flexibility within the protein. Figure 6 shows the  $R_2/R_1$  ratios for HdeA at all four pH values and Table II summarizes the correlation times ( $\tau_c$ ) (that can be estimated from the average  $R_2/R_1$  values (minus 10% outliers) using Eq. (3). Although there is some variation, the  $\tau_c$  values are consistent from one pH to another, with an average of  $10.22 \pm 0.54$  ns. This value matches well with the theoretical correlation time for the HdeA dimer, calculated by HydroPro<sup>13</sup> using the crystal structure (see Table II and Discussion).<sup>6</sup>

## Discussion

### Use of citrate buffer throughout the pH titrations

Citrate has the ability to buffer over the pH range 2.06–6.40; it was therefore the optimal buffer choice for our titration experiments performed between pH 3.0 and 6.0. Some previous experiments on HdeA

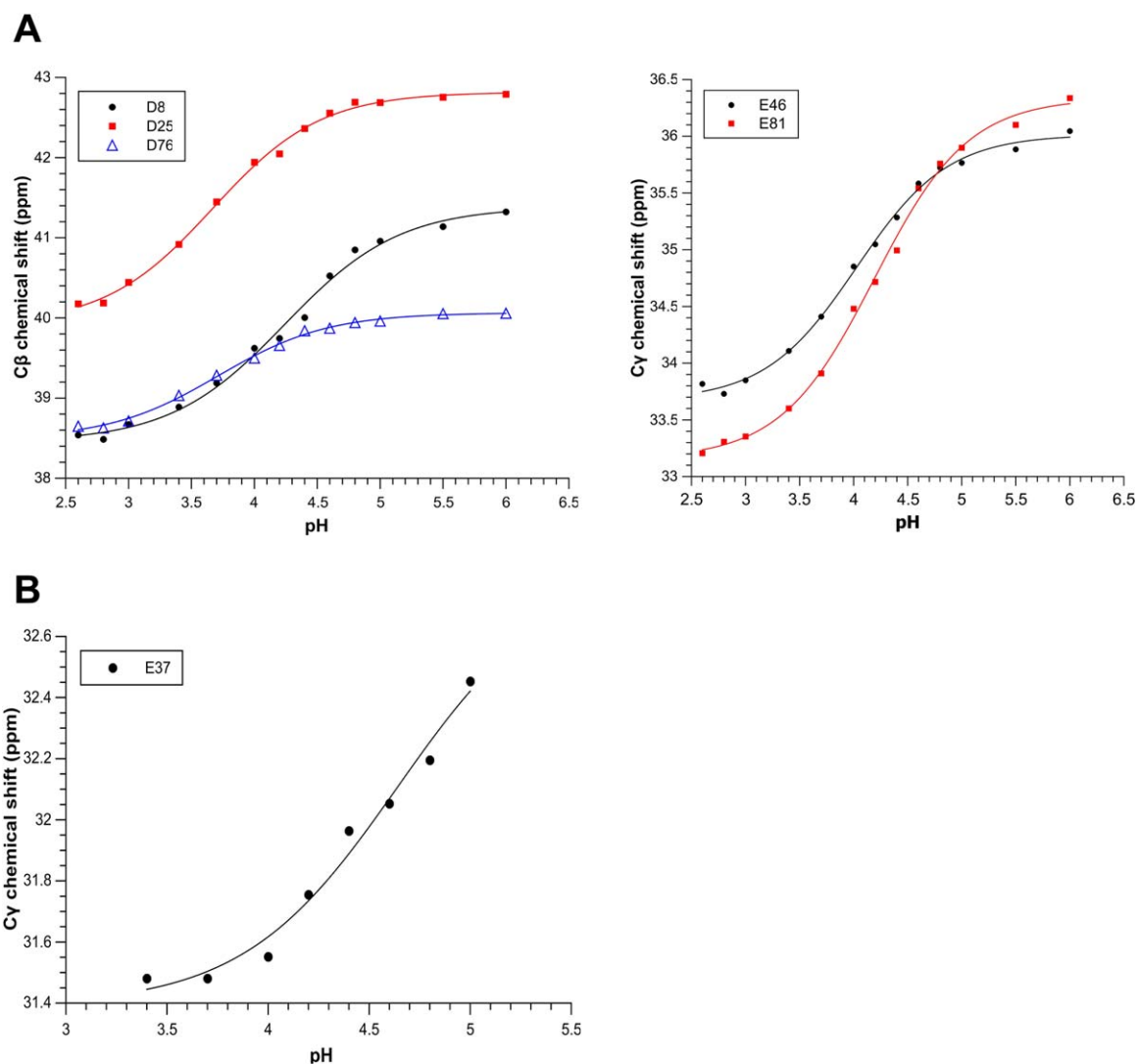


**Figure 4.** Sample fits of Asp and Glu  $pK_a$  data. A: Examples of well-fit Asp and Glu  $pK_a$  curves, monitoring  $^{13}C\beta$  and  $^{13}C\gamma$  chemical shifts, respectively, as a function of pH. B: Titration curve for E37, illustrating the absence of an upper plateau in the sigmoidal curve, thereby making curve fitting inaccurate for this residue.

have either utilized different buffers at each pH data point or buffers significantly outside their buffering capacities.<sup>2,6,9</sup> This is not ideal, especially in a case like this where the pH range monitors conformational as well as ionization changes for HdeA. Each buffer can affect the structure and therefore ionization of HdeA differently, and as such it would be difficult to compare results from each pH when the solution conditions are not the same. In order to maintain consistent salt content for each buffer, the HdeA sample was transferred to each new pH value via spin column rather than directly adding acid or base. This also ensured that the pH of the sample was accurate and not simply estimated.

#### **Amide chemical shift changes from pH 6.0 to 3.0 dominated by Asp and Glu protonation**

It was mentioned previously that only eight residues (A6, V13, N14, T17, N40, V49, G54, and I85) that have large chemical shift changes are also nonioniz-

able and not directly adjacent to an Asp or Glu residue in the sequence. Of these, G54 and I85 exhibit the largest overall shifts. In fact, their  $\Delta_{avg}$  values [defined by Eq. (1)] are more than three standard deviations ( $3\sigma$ ) above the mean shift (Fig. 3). However, upon examining the tertiary structure of HdeA it becomes clear that these large shifts are still primarily influenced by the ionization state of nearby residues: I85 is surrounded by lysines, at least one of which is involved in an intramonomer interaction with D51 at the N-terminus of helix C. It is likely that the large chemical shifts seen in 54 and 85 are due to alterations in the helix interactions and/or helix positions caused by the change in ionization state nearby. It supports evidence from other experiments of an overall loosening of the structure as the pH decreases (see discussion of hydrogen exchange and relaxation data, below). Similarly, residues A6, V13, N14, and T17 are all directly across from Asp and Glu residues within the folded protein, so their

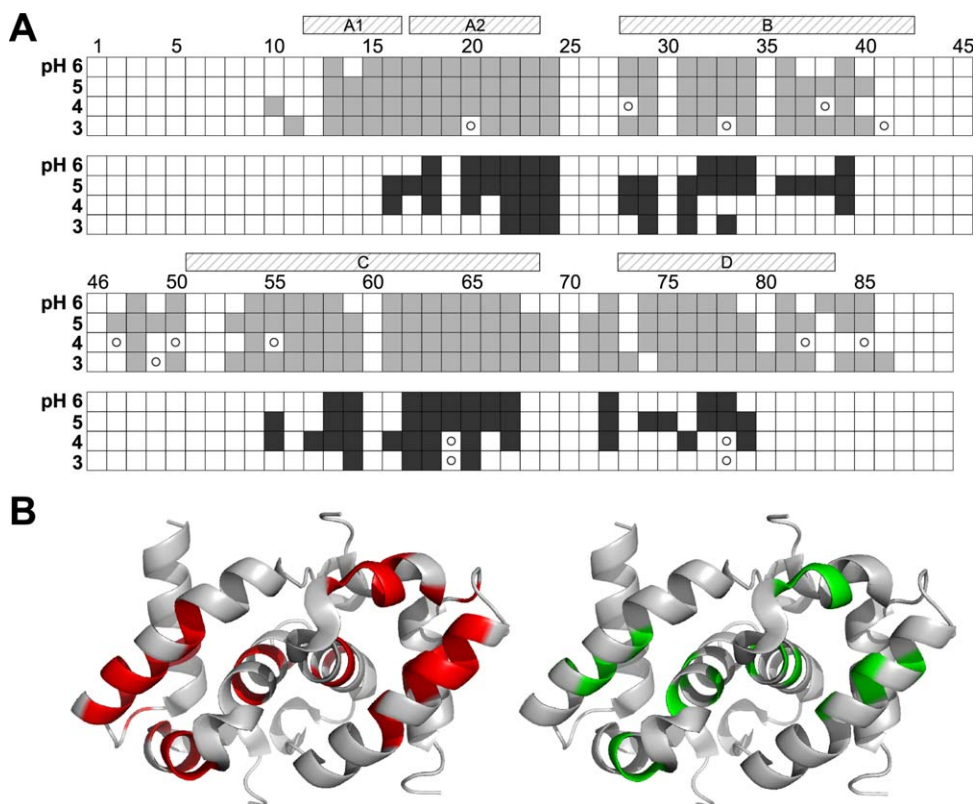


**Figure 5.** Summary of  $^1\text{H}/^2\text{H}$  exchange experimental results over the pH range 6.0–3.0. A: Gray boxes represent HdeA residues whose peaks were observable at that specific pH in a  $^1\text{H}$ - $^{15}\text{N}$  HSQC spectrum immediately after the protein was exchanged into deuterated buffer (after  $\sim 20$ – $25$  min). Black boxes correspond to residues at a particular pH for which peaks were still observable at the end of the exchange experiment (after  $\sim 12$  h). Open circles represent positions where the presence or absence of the peak is ambiguous due to overlap. Hatched bars above the data indicate the location of helices A–D within the folded protein. B: Residues that are still protected after 12 h at pH 6 (left, colored red) and pH 3 (right, colored green), mapped onto the structure of the folded dimer.

large average shifts are most likely dominated by conformational rearrangement caused by ionization changes as well. It has been previously proposed that non-ionizable residues whose  $^1\text{H}_\text{N}$  resonances undergo a  $>0.2$  ppm upfield shift and have a  $\text{pH}_{\text{mid}}$  within 0.2 units of the  $\text{pK}_\text{a}$  of a nearby Asp or Glu residue are likely to be involved in hydrogen bonding with the carboxylic group.<sup>14</sup> After analyzing our data, however, none of these eight residues fulfill this requirement, and therefore it is unlikely that the large shifts are due to hydrogen bonding with an aspartate or glutamate side chain.

Interestingly, several Asp and Glu residues (especially D20 and E81) show very small amide (and sometimes  $^{13}\text{C}_\beta$  or  $^{13}\text{C}_\gamma$ ) chemical shift changes between pH 6.0 and 3.0. The reason for the small overall shift change is often due, in part, to non-linear titration trajectories (data not shown). These non-linear curves provide evidence that some chemical shift changes reflect alterations in conformation that counteract the shifts due to changes in ionization state.

#### Comparing NMR-derived $\text{pK}_\text{a}$ data to simulations

The final two columns in Table I show the predicted  $\text{pK}_\text{a}$ s of the HdeA dimer and theoretical monomer from simulations by Brooks and co-workers, per-

formed using the constant pH molecular dynamics (CpHmd) technique.<sup>7</sup> When comparing the NMR-derived and the CpHmd-simulated data it was surprising to see that the monomer simulation more closely matches the experimental data than that of the dimer. In fact, the average difference between the NMR-derived  $\text{pK}_\text{a}$ s and the simulated dimer values is 0.65 pH units, whereas the average difference is only 0.31 to the (theoretical) monomer. In both the simulated monomer and dimer most of the  $\text{pK}_\text{a}$  values are underestimated compared with the NMR data.

The absence of the N- and C-terminal residues in the PDF (due to missing electron density in the crystal structure) may have had an effect on the simulated values for Asp and Glu amino acids found in the vicinity of these termini in the folded structure. Of the ionizable acidic side chains with the largest differences between the simulated and experimental data (D20, D43, D51, and D76), both D20 and D51 (in chain A) are directly across from the N-terminal residues (in chain B) that are missing in the simulation. This could help, in part, to explain the inaccuracy of the simulated  $\text{pK}_\text{a}$ s for these residues in the dimer, but does not explain why the simulated monomer value is a closer match to the experimental data.

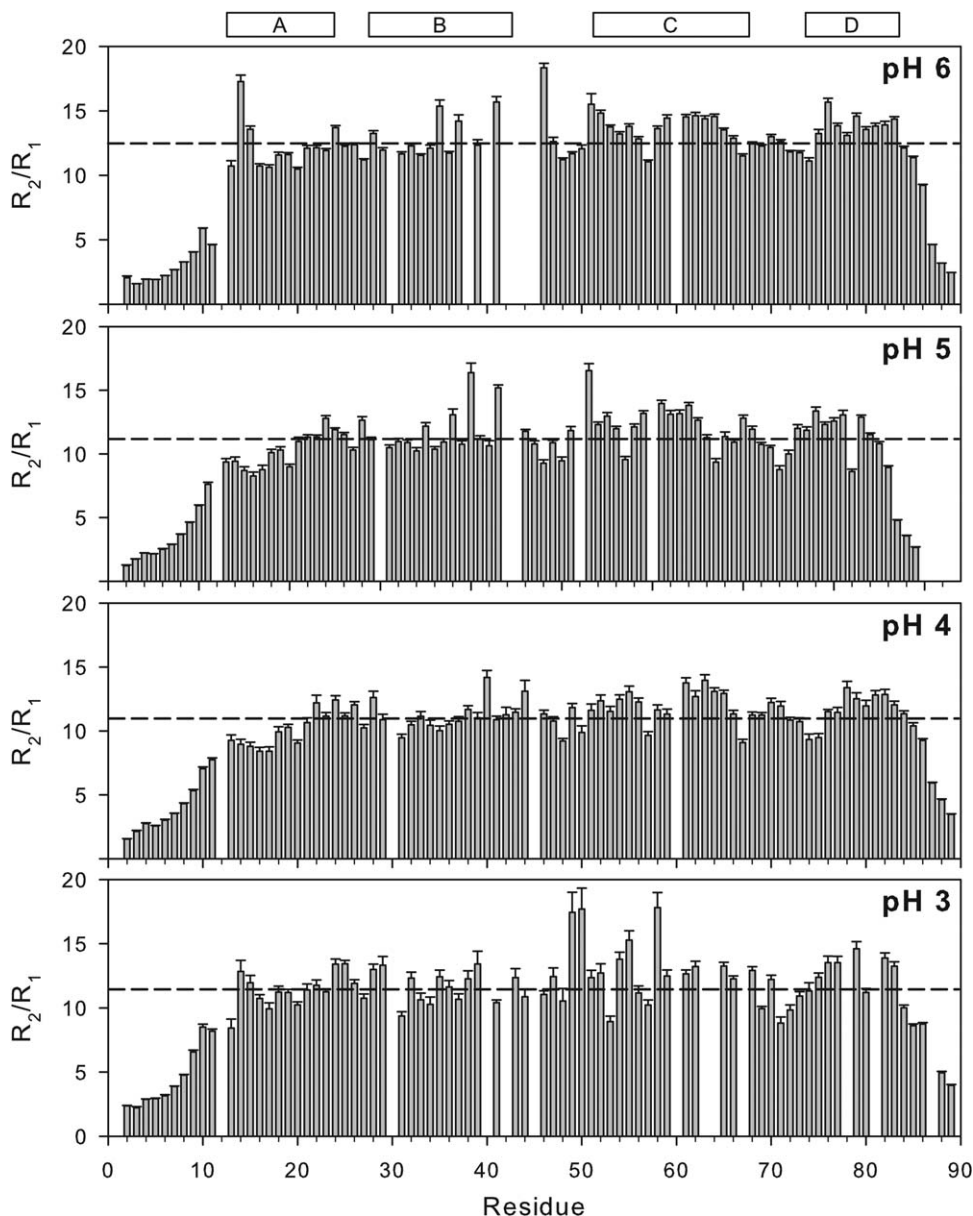


**Figure 6.**  $R_2/R_1$  ratios at each pH as a function of residue number. The pH at which the  $R_2$  and  $R_1$  data were recorded is indicated on each bar graph. The dashed horizontal lines indicate the average  $R_2/R_1$  ratio value at each pH (excluding 10% outliers). The rectangles at the top indicate the positions of helices A–D in the sequence. Very low ratio values indicate significant fast timescale backbone dynamics, while values substantially higher than the average  $R_2/R_1$  ratio suggest intermediate timescale motions at those residue positions.

The most significant reason for the differences between experimental and simulated results is likely due to the setup and methods used in the simulations. The simulation paper used short single runs over a pH range to obtain the population of unprotonated acidic groups and then fit the data to Henderson-Hasselbalch curves.<sup>7</sup> This technique has been since replaced by a method called pH-replica exchange (C.L. Brooks III, personal communication). The closer agreement between experimental and simulated monomer data may be explained by the techniques used, but may also be consistent with the idea that the protein is sampling more open conformations that are not being captured in the simula-

tion. This does not necessarily signify that the protein is sampling the monomer to any real extent at these pH values, but it may indicate that the protein becomes more conformationally dynamic and therefore the experimentally determined  $pK_a$ s are closer to random coil values than may be predicted from a dimer model with fewer conformations. By using more sampling and the newer pH-replica exchange technique in future simulations, the agreement with experimental results should be improved, and should better reflect transient structure-opening events that may be taking place (as predicted by hydrogen/deuterium exchange and relaxation data, see below).



**Table II.** Experimentally and Theoretically Determined Correlation Times at 25°C

pH	Experimental $\tau_c$ (ns) <sup>a</sup>	Estimated MW (kDa) <sup>b</sup>
6	10.69 ± 0.18	17.5
5	10.03 ± 0.22	16.4
4	9.99 ± 0.31	16.4
3	10.18 ± 0.40	16.7

HydroPro	Calculated $\tau_c$ (ns)	MW of input PDB structure (kDa)
Unmodified 1DJ8 dimer structure	9.74	17.5 <sup>c</sup>
“Rebuilt” 1DJ8 dimer structure <sup>d</sup>	10.59	19.5
“Rebuilt” 1DJ8 monomer structure <sup>d</sup>	5.96	9.7

<sup>a</sup>  $\tau_c$  values reported at pH 6.0–3.0 obtained from  $R_2/R_1$  ratios, following Eq. (3).

<sup>b</sup> Molecular weights for experimental data calculated using calibration data from the NorthEast Structural Genomics consortium wiki.<sup>28</sup>

<sup>c</sup> Molecular weight for crystal structure dimer, calculated using residues 9–87 (the positions that are visible).

<sup>d</sup> PDB file used for these HydroPro<sup>13</sup> calculations obtained by building residues 1–8 and 88–89 into the crystal structure coordinates using Swiss-PdbViewer.<sup>15</sup>

### Hydrogen/deuterium exchange experiments show a loosened but folded structure with reduced pH

Although our NMR spectra (Fig. 2) and some previous studies<sup>2</sup> show definitively that HdeA is still folded at pH 3.0, the results presented in this article also provide clear evidence that the protein is undergoing an overall unraveling of tertiary structure as the pH decreases and as the Asp and Glu side chains become neutralized, most likely in preparation for unfolding below pH 3.0. Even more interesting is the accelerated disappearance of spectral peaks during hydrogen/deuterium exchange, at pH values as high as 4.0, corresponding to residues in helix B (which is located in the interface of the HdeA dimer) (Fig. 5). The results indicate that, as the pH transitions to 4.0 and lower (and progressively falls below the  $pK_a$ s for aspartate and glutamate residues), the protein samples a larger range of conformations as a precursor to unfolding and transitioning to the monomer. Based on these results it appears that the dimer interface is one of the first segments within the HdeA dimer to start opening up, as shown by the large loss of solvent protection for helix B at pH 4.0.

It is also notable that the protein is slightly less protected at pH 6.0 compared to pH 5.0 (Fig. 5 and Supporting Information S1b). This is possibly a result of the ionization state of E37 in the center of the interface: given the estimated  $pK_a$  of E37 (at a value > 5.0) a significant proportion of HdeA molecules will have a charged E37 side chain at pH 6.0, possibly destabilizing the dimer structure and resulting in more conformational exchange. This is supported by the observation of broadened peaks for residues in the region of 38–44, indicating intermediate exchange (on an NMR chemical shift time-scale) in that segment of the folded structure at pH 6.0. It has already been proposed that the elevated  $pK_a$  for E37 also helps to force HdeA to release

bound substrates when the periplasmic environment returns to neutral pH.<sup>7</sup>

### Correlation times at each pH and comparison to theoretical values confirm that HdeA is a dimer throughout the pH range

It is clear from the experimental results (shown in Fig. 6 and Table II) that HdeA maintains its dimer structure at pH values down to 3.0 (and possibly lower), since the correlation times determined at each pH from  $R_2/R_1$  ratios fall within a relatively narrow range of values ( $10.22 \pm 0.54$  ns). In addition, those  $\tau_c$  values are all significantly higher than the expected correlation time for the monomer, which is estimated from HydroPro to be 5.96 ns.<sup>13</sup> The small decrease in  $\tau_c$  in moving from pH 6.0 to 5.0 supports data from the hydrogen/deuterium exchange experiments, in that the dimer seems to be slightly less compact at the higher pH, possibly due to the presence of the negatively charged E37 residue in the center of the interface (that becomes neutralized at pH 5.0). HydroPro was also used to calculate the expected correlation time for the dimer and monomer.<sup>13</sup> When using the original crystal structure (1DJ8) as the template,<sup>6</sup>  $\tau_c$  was significantly underestimated because 10 out of 89 residues are missing from the structure due to disorder at the N- and C-termini. We used Swiss-Pdb Viewer<sup>15</sup> to roughly build the missing residues into the crystal structure and re-run HydroPro. It is clear from the values in Table II that the rebuilt structure, containing the correct number of residues, better approximates the expected correlation time of the dimer.

We had some concerns that the maintenance of a folded dimer structure at pH 3.0 may be primarily an artifact of the high protein concentrations used for NMR studies. However, we see no evidence in the <sup>1</sup>H-<sup>15</sup>N HSQC spectra for unfolding or dissociation, even at very low HdeA concentrations (~20  $\mu$ M); in

fact, the spectra at high and low concentrations are identical (see Supporting Information Fig. S2).

### ***R<sub>2</sub>/R<sub>1</sub> ratios from relaxation studies support hydrogen/deuterium exchange experiments***

The  $R_2/R_1$  profiles at pH 5.0 and 4.0 are relatively uniform within the structured region of the protein, suggesting that residues in the helices are not participating in significant fast (ps–ns) or intermediate ( $\mu$ s–ms) timescale motions. Although the correlation time at pH 3.0 is similar to the values at pH 5.0 and 4.0, the plot of  $R_2/R_1$  as a function of residue (Fig. 6) illustrates an increase in the heterogeneity of the internal dynamics compared to the higher pHs. This supports the idea of a loosened tertiary fold while still maintaining the dimer.

The loop between helices B and C (BC loop) is the primary site at which we see evidence for intermediate timescale dynamics (signified by  $R_2/R_1$  ratio values that are at least 2 standard deviations ( $2\sigma$ ) higher than the trimmed mean). These motions are evident over the whole pH range, although interestingly, the exact sequence positions vary from one pH to another. At pH 6.0 residues N14 and E46 are likely to have  $\mu$ s–ms timescale motions. They are found directly across from each other on separate chains within the dimer, at the start of helix A and in the BC loop, respectively. We previously observed (when performing chemical shift assignment) that the BC loop region showed evidence for flexibility at pH 6.0 that resulted in peak broadening;<sup>16</sup> if peaks for residues 42–44 were visible in the spectra at this pH we may have also measured intermediate timescale motions at those positions. It appears that, at pH 6.0, the increased dynamics in the BC loop may induce similar motions at position 14 in helix A. At pH < 6.0, it is possible that conformational changes within the protein weaken the interaction between helix A and the BC loop, since  $\mu$ s–ms timescale dynamics are not seen at position 14 at the lower pH values. Other evidence for changes in the position and/or motions of the BC loop is seen by the fact that the amide peaks for five of the loop residues are missing from the HSQC at pH 6.0, but they become resolved at lower pH values, suggesting a change in the timescale of conformational exchange within the loop. At pH 5.0 the  $R_2/R_1$  ratios provide evidence that residues N40, D43, and Q53 are likely to exhibit intermediate timescale motions. These residues are all within or just peripheral to the BC loop, but have no direct interactions with each other. There is little evidence for intermediate motions at pH 4.0, which seems to run counter to the observation of a loosening structure that we see from the hydrogen/deuterium exchange experiments. It should be noted, however, that a “looser” structure is not necessarily more dynamic—it may just indicate that the structure is more opened up and therefore more solvent

exposed. Alternatively, the timescale at which we see loosening of the structure within the hydrogen exchange experiments may be much slower than can be observed using relaxation experiments. Residues V49, L50, and V58 show evidence for intermediate timescale backbone motions at pH 3.0, the first two of which are within the BC loop. Residue 58 lies at the center of helix C and would not be expected to display  $\mu$ s–ms motions; however, it is located directly across from E81 on helix D, and may therefore be reflecting some interhelical rearrangements that are occurring at the lowered pH due to charge neutralization (which are also reflected in large backbone chemical shift changes at G54 and I85, mentioned earlier).

One final item of note from the relaxation experiments is that residues 9–11 seem to become progressively more structured with decreased pH: the  $R_2/R_1$  ratio values transition from an average of 4.9 at pH 6.0–7.8 at pH 3.0. This agrees with the observation of increased solvent protection from residues 10 and 11 at pH 4.0 and 3.0 (Fig. 5), and our ability to measure protection factors for residues below position 11 at pH 4.0 and 3.0 (Supporting Information Fig. S1a). This observation seems somewhat unusual, given that residues 10 and 11 are both lysines, which are involved in stabilizing electrostatic interactions with D20 at higher pHs.<sup>9</sup> More work must be done to explain how the backbone amides of these lysine residues may be more structured after D20 is neutralized and the electrostatic interactions between the side chains are lost.

### **Summary**

We have clearly shown that HdeA maintains its dimer structure down to at least pH 3.0. Within this folded dimer framework, however, we have observed evidence (from hydrogen/deuterium exchange and relaxation experiments) for shifts in conformation and/or flexibility that have loosened the tertiary and quaternary structures, due primarily to the neutralization of side chain charge from aspartates and glutamates. The experimentally measured pK<sub>a</sub>s indicate that all Asp and Glu residues are well-protonated by pH 3.0; if the unfolding and dissociation processes were completely reliant on this change in ionization state we would have already expected to see dimer dissociation and more extensive unfolding by pH 3.0 in the titration. The neutralization of charge may have primed the protein for unfolding, but the stability of the folded dimer is clearly not dependent solely on charged aspartate and glutamate side chains. The next stage of these studies, therefore, will continue the pH titration from 3.0 to 2.0 in pursuit of a detailed analysis of the unfolding and activation process and the driving force behind the final transition to chaperone activity. Increased understanding of the mechanism of HdeA chaperone activation will permit improved targeting of this protein by therapeutics

that are intended to lower the infectivity of pathogenic bacterial strains.

## Materials and Methods

### Protein expression and purification

Expression and purification protocols for [U-<sup>13</sup>C,<sup>15</sup>N] labeled HdeA have been detailed in a previous publication.<sup>16</sup> In order to eliminate chemical shift variation due to changes in buffer type, all samples for the pH titration experiments utilized 50 mM citrate buffer, 10% <sup>2</sup>H<sub>2</sub>O and 0.4 mM DSS (2,2-dimethyl-2-silapentane-5-sulfonate, for chemical shift referencing), unless otherwise stated. For each pH in the titration the protein sample was exchanged into the new buffer using a spin column (2 mL Zeba spin column, 7 kDa MWCO, Thermo Scientific).

### NMR experiments

All experiments were recorded at 25 °C on an Agilent DD2 600 MHz NMR spectrometer with a room-temperature probe. Sample concentrations ranged from ~1.0 to 1.7 mM. Data were processed using NMRPipe/NMRDraw v.7.2<sup>17,18</sup> and spectra were analyzed with NMRViewJ v.9.0.<sup>19,20</sup> Curve fitting was performed using NMRViewJ and QtiPlot.<sup>21</sup>

<sup>1</sup>H-<sup>15</sup>N HSQC spectra were recorded on HdeA at pH 3.0, 3.4, 3.7, 4.0, 4.2, 4.4, 4.6, 4.8, 5.0, 5.5, and 6.0 to monitor backbone amide chemical shift change. HNCaCb and CbCa(CO)NH chemical shift assignment experiments were also recorded at pH 3.0, 4.0, 5.0, and 6.0 in order to ensure proper tracking of the movement of each assigned peak. Weighted averages of the overall backbone amide (<sup>1</sup>H<sub>N</sub> and <sup>15</sup>N) chemical shift changes between pH 6.0 and 3.0 were calculated using Eq. (1):

$$\Delta_{avg} = \sqrt{\frac{(\Delta H_N)^2 + \left(\frac{\Delta N}{5}\right)^2}{2}} \quad (1)$$

3D TOCSY (C(CO)NH) spectra were recorded at pH 2.6 and 2.8 in addition to the above listed pH values to measure Asp and Glu pK<sub>a</sub>s.<sup>22</sup> Titration curves (from plots of chemical shift as a function of pH for each residue) were fit to a modified Henderson-Hasselbalch equation:

$$y = a - \frac{a}{1 + 10^{(n(pK_a - pH))}} + \frac{b}{1 + 10^{(n(pK_a - pH))}} \quad (2)$$

where *a* and *b* are the minimum and maximum chemical shift values for the curve, respectively, and *n* is the Hill coefficient. When fitting data to obtain pK<sub>a</sub>s, the pH values were corrected by 0.04 units to account for the 10% <sup>2</sup>H<sub>2</sub>O in solution.<sup>23</sup>

Hydrogen exchange experiments were performed by rapid exchange of an HdeA sample from

citrate buffer in <sup>1</sup>H<sub>2</sub>O into 100% <sup>2</sup>H<sub>2</sub>O. At each pH, 72 x <sup>1</sup>H-<sup>15</sup>N SOFAST HSQC spectra were recorded sequentially, with each spectrum running for 9 min 37 s. Decay curves were fit with a standard exponential decay equation to obtain the observed rate of exchange for each amide group (*k*<sub>observed</sub>), and protection factors were obtained using the equation PF = (*k*<sub>intrinsic</sub>/*k*<sub>observed</sub>), where *k*<sub>intrinsic</sub> values were obtained from estimations calculated by the online program SPHERE.<sup>24,25</sup>

Backbone <sup>15</sup>N longitudinal (*R*<sub>1</sub>) and transverse (*R*<sub>2</sub>) relaxation rate constants were recorded on HdeA at pH 3.0, 4.0, 5.0, and 6.0 using standard <sup>1</sup>H-<sup>15</sup>N correlation experiments.<sup>26</sup> *R*<sub>1</sub> values were determined from 14 spectra with eleven delays of 0.01 (x3), 0.05, 0.10, 0.15, 0.20 (x2), 0.25, 0.30, 0.40, 0.50, 0.60, and 0.80 s. *R*<sub>2</sub> values were obtained from twelve spectra with nine delays of 0.01 (x2), 0.03 (x2), 0.05, 0.07, 0.09 (x2), 0.11, 0.13, 0.15, and 0.17 s. The correlation time (*τ*<sub>c</sub>, in s) at each pH was estimated from 10% trimmed, averaged *R*<sub>2</sub>/*R*<sub>1</sub> ratios using Eq. (3):

$$\tau_c \sim \frac{1}{4\pi\nu_N} \sqrt{6\frac{R_2}{R_1} - 7} \quad (3)$$

where *ν*<sub>N</sub> is the <sup>15</sup>N resonance frequency (60 786 494 Hz, in our case). The equation was derived from Kay et al.<sup>27</sup> and the NESG Wiki online.<sup>28</sup> HydroPro<sup>13</sup> was used to calculate the expected correlation time, based on a “rebuilt” crystal structure: since the reported crystal structure (1DJ8)<sup>6</sup> was missing 8 amino acids from the N-terminus and 2 from the C-terminus, we used Swiss-Pdb Viewer to build the missing residues onto the structure and then perform a basic minimization<sup>15</sup> in order to provide a rough structure with a size more comparable to the full-length dimer that could be used for modeling.

## Acknowledgments

The authors would like to thank Drs. Charles Brooks III and Voula Kanelis for helpful insights into the interpretation of our data, and Dr. James Bardwell for providing the HdeA plasmid. This article is dedicated to the memory of Dr. Paul Shin, whose unflinching enthusiasm and determination were key factors in our ability to obtain an NMR spectrometer and to drive our research forward.

## References

1. Wu YE, Hong W, Liu C, Zhang L, Chang Z (2008) Conserved amphiphilic feature is essential for periplasmic chaperone HdeA to support acid resistance in enteric bacteria. *Biochem J* 412:389–397.
2. Hong W, Jiao W, Hu J, Zhang J, Liu C, Fu X, Shen D, Xia B, Chang Z (2005) Periplasmic protein HdeA exhibits chaperone-like activity exclusively within stomach

- pH range by transforming into disordered conformation. *J Biol Chem* 280:27029–27034.
3. Black RE, Cousens S, Johnson HL, Lawn JE, Rudan I, Bassani DG, Jha P, Campbell H, Walker CF, Cibulskis R, Eisele T, Liu L, Mathers C, Child Health Epidemiology Reference Group of WHO, Unicef (2010) Global, regional, and national causes of child mortality in 2008: a systematic analysis. *Lancet* 375:1969–1987.
  4. Koebnik R, Locher KP, Van Gelder P (2000) Structure and function of bacterial outer membrane proteins: barrels in a nutshell. *Mol Microbiol* 37:239–253.
  5. Schirmer T (1998) General and specific porins from bacterial outer membranes. *J Struct Biol* 121:101–109.
  6. Gajiwala KS, Burley SK (2000) HDEA, a periplasmic protein that supports acid resistance in pathogenic enteric bacteria. *J Mol Biol* 295:605–612.
  7. Zhang BW, Brunetti L, Brooks CL, III (2011) Probing pH-dependent dissociation of HdeA dimers. *J Am Chem Soc* 133:19393–19398.
  8. Tapley TL, Korner JL, Barge MT, Hupfeld J, Schauerte JA, Gafni A, Jakob U, Bardwell JC (2009) Structural plasticity of an acid-activated chaperone allows promiscuous substrate binding. *Proc Natl Acad Sci USA* 106:5557–5562.
  9. Foit L, George JS, Zhang BW, Brooks CL, III, Bardwell JC (2013) Chaperone activation by unfolding. *Proc Natl Acad Sci USA* 110:E1254–E1262.
  10. Tapley TL, Franzmann TM, Chakraborty S, Jakob U, Bardwell JC (2010) Protein refolding by pH-triggered chaperone binding and release. *Proc Natl Acad Sci USA* 107:1071–1076.
  11. Roux-Fromy M (1982) On the Hill plot of NMR data for titration of protein residues. *Biophys Struct Mech* 8:289–306.
  12. Song J, Laskowski M, Jr, Qasim MA, Markley JL (2003) NMR determination of pK<sub>a</sub> values for Asp, Glu, His, and Lys mutants at each variable contiguous enzyme-inhibitor contact position of the turkey ovomucoid third domain. *Biochemistry* 42:2847–2856.
  13. Ortega A, Amoros D, Garcia de la Torre J (2011) Prediction of hydrodynamic and other solution properties of rigid proteins from atomic- and residue-level models. *Biophys J* 101:892–898.
  14. Castaneda CA, Fitch CA, Majumdar A, Khangulov V, Schlessman JL, Garcia-Moreno BE (2009) Molecular determinants of the pK<sub>a</sub> values of Asp and Glu residues in staphylococcal nuclease. *Proteins* 77:570–588.
  15. Guex N, Peitsch MC (1997) SWISS-MODEL and the Swiss-PdbViewer: an environment for comparative protein modeling. *Electrophoresis* 18:2714–2723.
  16. Crowhurst KA (2013) <sup>13</sup>C, <sup>15</sup>N and <sup>1</sup>H backbone and side chain chemical shift assignment of acid-stress bacterial chaperone HdeA at pH 6. *Biomol NMR Assign* DOI: 10.1007/s12104-013-9508-0.
  17. NMRPipe/NMRDraw, Version 7.5. North Potomac, MD: NMR Science; 2012.
  18. Delaglio F, Grzesiek S, Vuister GW, Zhu G, Pfeifer J, Bax A (1995) NMRPipe: a multidimensional spectral processing system based on UNIX pipes. *J Biomol NMR* 6:277–293.
  19. Johnson BA (2004) Using NMRView to visualize and analyze the NMR spectra of macromolecules. *Methods Mol Biol* 278:313–352.
  20. NMRViewJ, Version 9.0. Newark, NJ: One Moon Scientific, Inc.; 2013.
  21. QtiPlot, Version 0.9.9-rc7. Craiova, Romania: ProIndep Serv SRL; 2013.
  22. Grzesiek S, Anglister J, Bax A (1993) Correlation of backbone amide and aliphatic side-chain resonances in <sup>13</sup>C/<sup>15</sup>N-enriched proteins by isotropic mixing of <sup>13</sup>C magnetization. *J Magn Reson Ser B* 101:114–119.
  23. Lindman S, Linse S, Mulder FA, Andre I (2007) pK(a) values for side-chain carboxyl groups of a PGB1 variant explain salt and pH-dependent stability. *Biophys J* 92:257–266.
  24. Bai Y, Milne JS, Mayne L, Englander SW (1993) Primary structure effects on peptide group hydrogen exchange. *Proteins* 17:75–86.
  25. SPHERE - A Server Program for Hydrogen Exchange Rate Estimation, Philadelphia, PA: Roder Lab; 1995.
  26. Farrow NA, Muhandiram R, Singer AU, Pascal SM, Kay CM, Gish G, Shoelson SE, Pawson T, Forman-Kay JD, Kay LE (1994) Backbone dynamics of a free and phosphopeptide-complexed Src homology 2 domain studied by <sup>15</sup>N NMR relaxation. *Biochemistry-US* 33:5984–6003.
  27. Kay LE, Torchia DA, Bax A (1989) Backbone dynamics of proteins as studied by <sup>15</sup>N inverse detected heteronuclear NMR spectroscopy: application to staphylococcal nuclease. *Biochemistry-US* 28:8972–8979.
  28. NMR determined rotational correlation time, University at Buffalo: NorthEast Structural Genomics Consortium (NESG); 2011.